Editor Choice paper

Adsorption modes of aromatic ketones on platinum and their reactivity towards hydrogenation

A. Vargas, S. Reimann, S. Diezi, T. Mallat, A. Baiker [*]

*Institute for Chemical and Bioengineering, Department of Chemistry and Applied Biosciences, ETH-Zürich,
Hönggerberg HCI, CH-8093 Zürich, Switzerland*

Abstract

Heterogeneous catalytic hydrogenation of ketones is an important synthetic route to alcohols, but the detailed reaction pathway of this common reaction is still unknown. In particular, different opinions exist concerning the nature of the surface intermediates that eventually react with the activated surface hydrogen: η^1(O) and η^2(C,O) adsorbed intermediates have been postulated by different authors, leading to different surface reaction pathways. Here we studied the hydrogenation of aromatic ketones activated by an ester group in α-position. Ethyl benzoylformate (**1**) was hydrogenated on Pt/Al$_2$O$_3$ under mild conditions, but insertion of one or two *o*-substituents into the aromatic ring diminished or completely eliminated the reactivity of the ketone. The dramatic difference between the reactivities of **1** and ethyl mesithylglyoxylate (**5**) prompted us to investigate the adsorption geometries and energies of the two ketones by electronic structure calculations on a model platinum (1 1 1) surface. The calculations revealed that the presence or absence of *o*-substitution on the phenyl ring strongly affects the interaction mode of the C=O moiety with the metal surface. In particular, *o*-substitution suppresses adsorption modes where the keto-carbonyl group is bound to the metal in η^2(C,O) mode. Following such observations the reactivity of aromatic ketones is discussed, and a correlation between adsorption mode and reactivity of the ketone towards hydrogenation is proposed that could be critical for the further investigation of a complete reaction mechanism.
© 2007 Elsevier B.V. All rights reserved.

Keywords: α-Keto esters; Aromatic ketones; Adsorption; Hydrogenation; Pt/Alumina; Metal cluster; DFT; Pt(1 1 1)

1. Introduction

The adsorption of ketones on transition metals has been the topic of many studies employing surface science techniques [1–5] typically in ultrahigh vacuum and consequently under *ex situ* conditions. Such experimental studies are often combined with density functional theory (DFT) calculations of the ketones on model surfaces aiming to unravel their interaction with the metal. This is often critical for the interpretation of the rate and the chemo- and enantioselectivity of hydrogenation reactions [6–8]. Previous to surface science techniques such topic had been addressed mainly by means of isotopic exchange and by studying the kinetic effects due to substitution [9,10]. In general, ketones adsorb on transition metal surfaces *via* two alternative bonding configurations: as η^1(O) in an end-on adsorption

configuration in which the oxygen atom is bonded by its lone pair orbital to the metal surface, or as η^2(C,O), with both the carbon and the oxygen atoms of the keto-group σ-bonded to the metal and the C=O moiety lying parallel to the surface. Thermal desorption spectra (TDS) and high-resolution electron energy loss vibrational spectroscopic (HREELS) studies of acetone on a Pt foil have shown evidence of both adsorption geometries [4]. On the basis of DFT electronic structure calculations and comparative studies on the rate of hydrogenation of acetone (non-activated ketone) and 1,1,1-trifluoroacetone (activated ketone), it was proposed that the η^2(C,O) adsorption mode could be the reactive intermediate for the hydrogenation of carbonyl compounds on platinum group metals [5]. The basic idea behind this proposal emerged from the following observations: (i) while acetone hardly reacted on platinum, 1,1,1-trifluoroacetone was quickly hydrogenated under the same reaction conditions, and (ii) acetone prefers an η^1(O) adsorption mode while 1,1,1-trifluoroacetone assumes a more stable η^2(C,O) adsorption mode. On the contrary, other authors pro-

[*] Corresponding author.
E-mail address: baiker@chem.ethz.ch (A. Baiker).

posed that the hydrogenation of acetone occurs via an $\eta^1(O)$ intermediate [7], in a similar fashion to what had been proposed for the hydrogenation of formaldehyde on Pt(1 1 1) [11]. Since the two proposals other studies have appeared, which are more consistent with the critical role of an $\eta^2(C,O)$ intermediate [12,13], but nonetheless a clear picture of the reaction pathway has not yet been obtained.

The preceding models are largely based on the comparison between catalytic data and DFT calculations, as well as high vacuum investigations. Adsorption geometries may be affected also by the reaction conditions including temperature, pressure, solvent, and concentrations [14], which are still difficult to model at a sufficiently accurate level of theory for real systems [15]. For the heterogeneous enantioselective hydrogenation of α-ketoesters over cinchona-modified Pt/Al$_2$O$_3$ it has been shown that depending on the modifier concentration various adsorption geometries of cinchonidine (*via* the quinoline ring) on Pt are feasible and the adsorption mode of the modifiers determines the outcome of enantioselective hydrogenation of the ketone [16]. Recently, it has been suggested for the enantioselective hydrogenation of ethyl pyruvate that the role of the modifier is to interact with the $\eta^1(O)$ adsorption mode of the substrate and tilt the substrate plane toward the surface to an $\eta^2(C,O)$ adsorption mode, in which hydrogenation of the keto-carbonyl group is possible [7]. Due to the fact that hydrogenation is also possible in the absence of chiral modifier, this flip from $\eta^1(O)$ to $\eta^2(C,O)$ should be ascribed as a property of the substrate itself. The adsorption behavior of methyl and ethyl pyruvate has already been investigated by many surface sensitive techniques such as XPS and UPS [17], XANES [18], STM [19], and NEXAFS [20].

Herein we report an intriguing new experimental observation in the hydrogenation of activated aromatic ketones, which suggests that there is an important steric requirement a ketone has to fulfill to be hydrogenated on Pt. DFT calculations on a model surface support the experimental results, thus providing interesting insight concerning the possible correlation between the adsorption mode of the ketones and their reactivity towards hydrogenation on platinum.

2. Experimental

2.1. Materials

Ethyl benzoylformate (**1**, 95%, Aldrich) and ethyl mesitylglyoxylate (97%, Alfa Aesar) **5** were carefully distilled in vacuum before use. Ethyl 3,5-dimethylbenzoylformate (**2**), ethyl naphthylglyoxylate (**3**) and ethyl anthracenylglyoxylate (**4**) were prepared by the reaction of the corresponding Grignard reagents with diethyl oxalate or ethyl chlorooxoacetate according to known methods in the literature [21,22]. All synthesized substrates were carefully purified using flash chromatography and their structure and purity were checked by GC, GC-MS, HPLC, and NMR. Acetic acid (AcOH, 99.8%, Fluka) was used as received and toluene (99.5%, J. T. Baker) was dried and stored over activated molecular sieve. The 5 wt% Pt/Al$_2$O$_3$ (E-4759) catalyst was purchased from Engelhard.

2.2. Catalytic hydrogenations

The hydrogenation reactions were carried out in a mechanically stirred eight parallel pressure reactor system (Argonaut Technologies) or in a magnetically stirred stainless steel autoclave controlled by a computerized constant-volume constant-pressure equipment (Büchi BPC 9901). The 5 wt% Pt/Al$_2$O$_3$ catalyst was pre-reduced before use in a fixed-bed reactor by flushing with N$_2$ at 400 °C for 30 min, followed by reductive treatment in H$_2$ for 60 min at the same temperature. After cooling to room temperature in H$_2$ (30 min), the catalyst was transferred to the hydrogenation reactor. According to standard conditions, 42 mg catalyst, 1.84 mmol substrate, and 5 ml solvent were stirred (1000 rpm) at 10 bar and room temperature (23–25 °C) for 2 h.

According to TEM measurements, the average particle size of Pt after the reductive heat treatment was 3.7 nm [23].

2.3. Analytics

Conversion was determined by a HP-6890 gas chromatograph equipped with a HP-5 (30 m × 0.32 mm × 0.25 μm) capillary column as well as by HPLC using a MERCK LaChrom system with a CHIRACEL OD column (4.6 mm i.d., 240 mm length, 10 μm particle size). The HPLC measurements were carried out at 10 °C with a liquid flow of 0.5 ml/min. The UV detector was set to 210 nm. For all substrates a mixture of *n*-hexane/isopropanol (9/1) was used as eluent. Products were identified by GC/MS (HP-6890 coupled with a HP-5973 mass spectrometer) and by ^{1}H and ^{13}C NMR. All NMR data were recorded on a Bruker Avance 500 with TMS as internal standard.

2.4. Computational methods

Adsorption studies have been performed using the Amsterdam Density Functional (ADF) program package [24] using a Pt 31 cluster to simulate the metal surface. A detailed description of the application of such cluster for adsorption studies has been published elsewhere [8,13,25,26] and we here give only some basic information on the model chemistry used. A frozen core approximation was used for the description of the inner core of the atoms. Orbitals up to 1s were kept frozen for the second row elements, while orbitals up to 4f were kept frozen for platinum. The core was modeled using a relativistically corrected core potential created with the DIRAC utility of the ADF program. Furthermore the relativistic scalar approximation (mass–velocity and Darwin corrections) was used for the Hamiltonian, with the zero order regular approximation (ZORA) formalism, where spin-orbit coupling is included already in zero order [27–31]. The ZORA formalism requires a special basis set, to include much steeper core-like functions, implemented in the code. Within this basis set the double-ζ (DZ) basis functions were used for platinum. For second row elements and hydrogen double-ζ polarized (DZP) basis functions were used. The local part of the exchange and correlation functional was modeled using a Vosko, Wilk, Nuisar parametrization of the electron gas

[32]. The non-local part of the functional was modeled using the Becke correction for the exchange [33] and the Perdew correction for the correlation [34]. All calculations were run unrestricted.

Structures and conformations of **1a** and **5a** were calculated with the Gaussian 03 set of programs [35], using density functional theory with a B3LYP hybrid functional [36–38] and the 6-31G (d,p) basis set of Pople and co-workers.

3. Results and discussion

3.1. Catalytic hydrogenation

The study of the mechanism of hydrogenation of ketones previous to surface science investigations has been addressed by means of isotope labeling and substituent effects [9,10]. Isotopic labeling points toward the predominant role of weakly bound species as effective hydrogenation intermediates, and substituent effects show that in general bulky groups are detrimental to the reaction rate of the hydrogenation reaction.

The hydrogenation of α-ketoesters to the corresponding alcohols has generated great interest since the first reports of Orito and co-workers [39,40] using cinchona-modified Pt. Hydrogenation of these activated ketones runs smoothly already under very mild conditions, either in the presence or absence of the alkaloid as chiral modifier [41–43]. Under the standard conditions used here (10 bar, room temperature) full conversion of **1** and **2** was achieved on Pt/Al$_2$O$_3$ within 2 h in the weakly polar toluene and the protic polar solvent acetic acid (Table 1). A considerable decrease in reactivity was observed in the hydrogenation of **3**. The naphthyl substituent in α-position

to the keto-carbonyl group decreased the conversion in both solvents. The lower reactivity may be explained by considering the larger size of active site ensembles necessary to accomodate the bulky α-ketoester **3**, and the presumably stronger adsorption of substrate and product on the metal surface. This explanation, however, does not hold for substrates **4** and **5**: no alcohol could be detected in the hydrogenation of these α-ketoesters. Although the hydrogenation of the anthracenyl derivative **4** may require a huge active site ensemble, the mesithyl derivative **5** is relatively small and a too strong adsorption on the Pt surface is not expected either. The main structural similarity in substrates **4** and **5** is the presence of two *o*-substituents in the phenyl ring, as compared to the structure of ethyl benzoylformate **1**.

Any attempt to convert **5** at ambient temperature failed. Hydrogenation under higher pressure (25 bar) and longer reaction time (8 h) did not lead to detectable formation of the alcohol product. To eliminate the possibility that some impurity in the substrate poisons the Pt catalyst and thus prevents the transformation, we repeated the reaction in Table 1 in the presence of half equivalent of ethyl pyruvate (0.6 mmol ethyl pyruvate and 1.2 mmol **5**). Ethyl pyruvate was transformed completely to ethyl lactate in 2 h, but **5** remained unreactive.
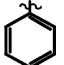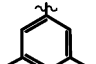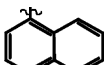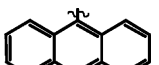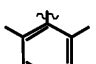
A feasible explanation for the non-reactivity of **4** and **5** is that the two aromatic substituents in *o*-position prevent a reactive adsorption mode of the keto-carbonyl group, and that in the absence of this intermediate on the Pt surface hydrogenation does not take place. This possibility is analyzed subsequently, using theoretical calculations.

3.2. Theoretical adsorption studies

In order to gain a better insight into the influence of adsorption modes on the reaction rate of ketone hydrogenation, we studied the theoretical adsorption modes of methyl benzoylformate (**1a**) and methyl mesithylglyoxylate (**5a**) on Pt. Note that **1a** and **5a** are used as models for **1** and **5**, respectively; the only difference being that the former two are methyl esters while the latter two are ethyl esters. Fig. 1 shows the computed structures in a vacuum of *s-cis* and *s-trans* **1a** and **5a**. For **1a** the *s-trans* conformation is more stable by 1.3 kcal/mol, while for **5a** the *s-cis* conformation is the preferred structure by 2.1 kcal/mol, at the level of theory used (for details, see the computational methods section). The reason for the change in the most stable conformer is the effect of the two *o*-methyl substituents on the phenyl ring that destabilizes the conjugation between the keto-carbonyl group and the aromatic moiety, and furthermore destabilizes the *s-trans* conjugation between the keto-carbonyl and the ester-carbonyl groups.

Figs. 2–5 show the adsorption modes of the two molecules on a Pt(1 1 1) surface. In the figures the C=O moiety of the adsorbed aromatic ketone has been highlighted with an arrow to focus the attention on the position of this moiety with respect to the surface. Table 3 shows the bond lengths of the keto- and ester-carbonyl moieties in all the structures depicted in Figs. 1–5. In all cases the aromatic moiety was adsorbed on the bridge site, since this has been shown to be the favorite adsorption geometry for benzene and in general for substituted aromatic systems on

Table 1

Hydrogenation of bulky α-ketoesters over Pt/Al$_2$O$_3$ in toluene and acetic acid (standard conditions)

Substrate	R	Conversion (%)	
		Toluene	AcOH
1		100	100
2		100	100
3		48	21
4		0	0
5		0	0

(1a)

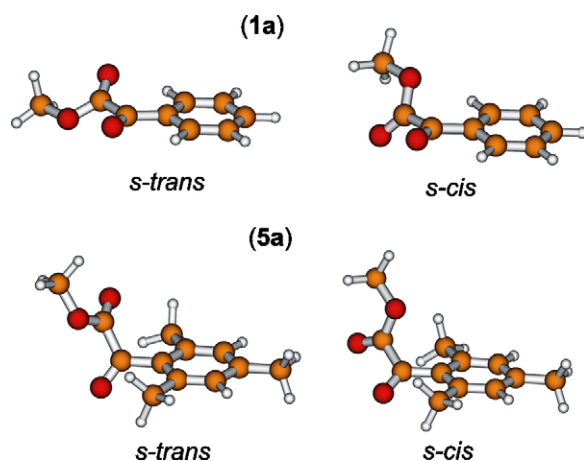*s-trans*   *s-cis*

(5a)

s-trans   *s-cis*

Fig. 1. Optimized structures of *s-trans* and *s-cis* methyl benzoylformate (**1a**) and methyl mesithylglyoxylate (**5a**). The *o*-substituents on the phenyl moiety disrupt the π system conjugation resulting in a more stable *s-cis* conformer for **5a**.

Pt(1 1 1) [8,44–47]. Due to the symmetry lowering of benzene on a bridge site [48], substitution can occur on apical or non-apical carbons (Fig. 2), giving rise to non-equivalent adsorbed structures. Furthermore, the relative stability between *s-cis* and *s-trans* conformers of the molecules in study could in principle not be reflected by the relative energies of adsorbed molecules, due to specific interactions with the metal sites, therefore for each of the two molecules both conformers had to be considered while studying the preferred adsorption mode. Due to these facts, although only two molecules were studied, the number of interesting surface structures to be considered was rather large.

For **1a**, the $\eta^2(C,O)$ adsorption modes are illustrated in Fig. 2. Only non-apical ring substitution resulted in $\eta^2(C,O)$ adsorption

of the keto-carbonyl moiety. Due to the greater re-hybridization of the apical carbon atom, apical substitution does not result in a chemisorption of the keto-carbonyl moiety. The adsorption of the phenyl ring dominates and the keto-carbonyl is too far from surface metal atoms to form chemisorption bonds. It is here clearly seen the importance of surface topology in the adsorption of multifunctional molecules. Adsorption tends to be dominated by one moiety, while optimal adsorption of another moiety depends on the geometrical disposition of the neighboring metal atoms, as already shown for acetophenone [8] and 1-phenyl-1,2-propanedione [13]. Adsorption energies (Table 2) calculated for the used level of theory, reveal that the *s-cis* non-apical adsorption mode is the most stabilized, while the other three structures have very similar adsorption energies.

Fig. 3 shows the $\eta^1(O)$ adsorption structures for **1a**. Only for apical structures local minima are found, while for non-apical substitution the geometries relax to $\eta^2(C,O)$ adsorption modes. The energies of such modes, as shown in Table 2, are significantly lower (by more than 10 kcal/mol) than the ones shown in Fig. 2, indicating that their fractional coverage should be very low or negligible. The oxygen atom of the carbonyl group is not interacting with metal atoms of the surface as in a typical $\eta^1(O)$ mode, but is rather constrained in the shown position by the mentioned re-hybridization of the apical carbon atoms.

When **5a** adsorption modes are considered (Figs. 4 and 5 and Table 2), the most striking result is that the adsorption energies decrease remarkably. In particular $\eta^2(C,O)$ adsorption modes (Fig. 4) are formed only for non-apical substitution, as seen for **1a**, while for the apical substitution the keto-carbonyl is pushed away from the surface and finally results pointing in the opposite direction from the metal. $\eta^1(O)$ adsorption modes (Fig. 5)

s-cis apical   *s-cis* non apical

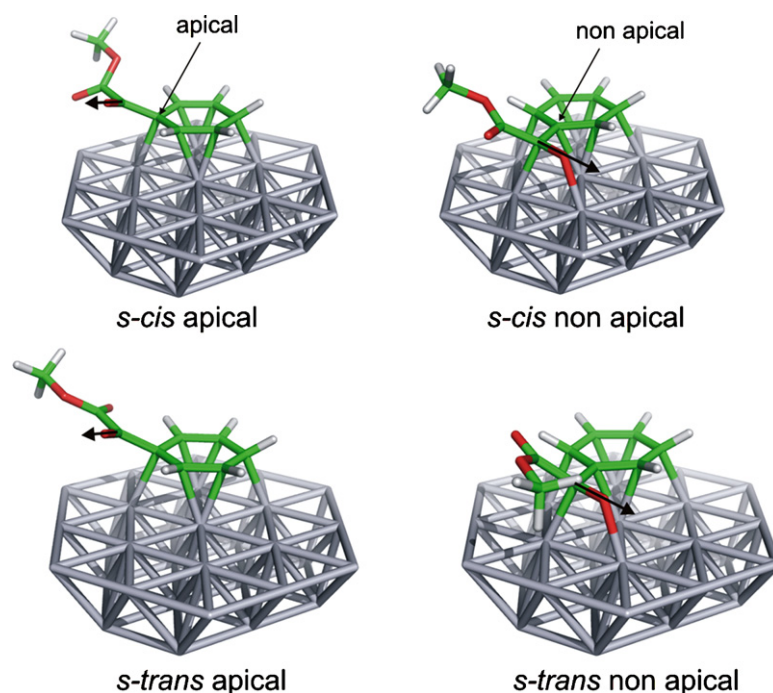*s-trans* apical   *s-trans* non apical

Fig. 2. η^2 adsorption modes of methyl benzoylformate (**1a**) on Pt(1 1 1). Position of the C=O moiety is highlighted by an arrow. Atom colors are: Pt—grey, C—green, O—red, H—light grey. (For interpretation of the references to color in this figure legend, the reader is referred to the web version of the article.)

Fig. 3. η^1 adsorption modes of methyl benzoylformate (**1a**) on Pt(1 1 1). Position of the C=O moiety is highlighted by an arrow. Atom colors are: Pt—grey, C—green, O—red, H—light grey. (For interpretation of the references to color in this figure legend, the reader is referred to the web version of the article.)
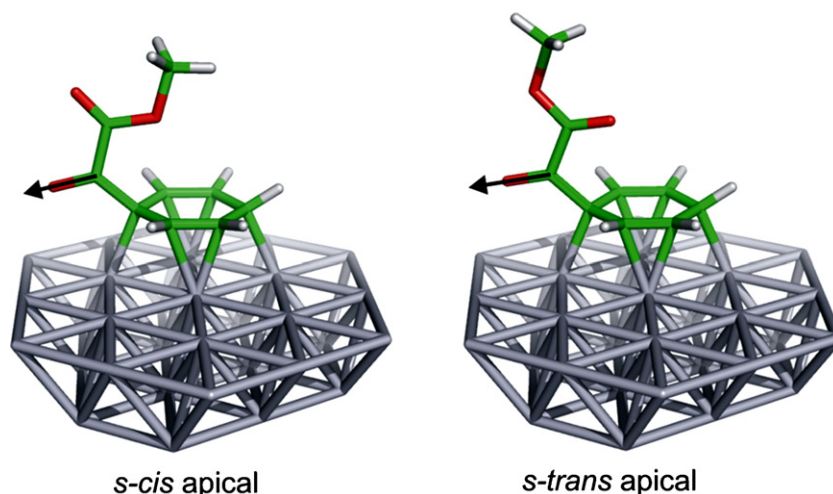
exist for all four cases, but with the distinction that only for non-apical substitution the surface topology allows formation of bonds between the C=O moiety and the metal. This is also clearly seen by the values of the C=O bond lengths (Table 3) that show elongation from 1.2 to 1.3 Angstrom only for non-apical substitution. In summary the presence of the two *o*-methyl substituents on the aromatic ring has the effect of destabilizing η^2(C,O) surface modes (Fig. 4, Table 2), and to trap the η^1(O) modes (Fig. 5) between the *o*-methyl substituents. In general, the described results are in agreement with the previously published ones concerning the structure of carbonyl groups on

platinum and the competition between the adsorption of different functional groups in the overall adsorption state of a complex molecule [8,11,13].

3.3. Ketone hydrogenation: correlation between adsorption mode and reactivity

As already noted in the introduction, two proposals exist in the literature concerning the role of intermediate chemisorption modes of ketones in hydrogenation reactions. According to one concept, the η^2(C,O) adsorption structure is the key reaction
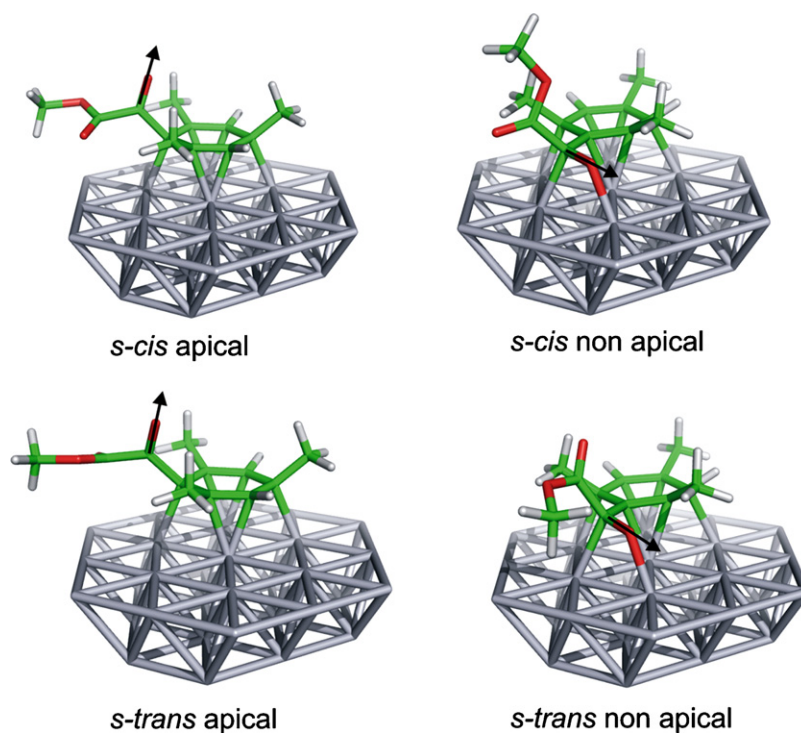

Fig. 4. η^2 adsorption modes of methyl mesithylglyoxylate (**5a**) on Pt(1 1 1). Note that for apical structures C=O is removed from η^2 adsorption and points away from the metal. Position of the C=O moiety is highlighted by an arrow. Atom colors are: Pt—grey, C—green, O—red, H—light grey. (For interpretation of the references to color in this figure legend, the reader is referred to the web version of the article.)

Fig. 5. η^1 adsorption modes of methyl mesithylglyoxylate (**5a**) on Pt(1 1 1). Position of the C=O moiety is highlighted by an arrow. Atom colors are: Pt—grey, C—green, O—red, H—light grey. (For interpretation of the references to color in this figure legend, the reader is referred to the web version of the article.)
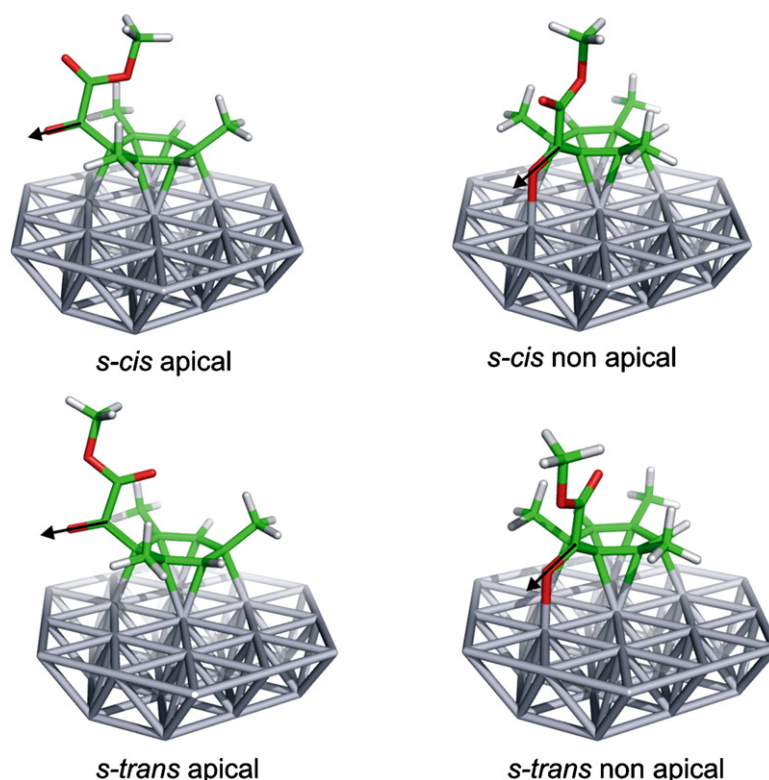
intermediate, whereas η^1(O) adsorption modes are spectators. In another model the opposite scenario is prospected [7,8]. Both proposals use modeling studies and experimental observations as arguments of support. The main arguments in favor of the first proposal are the following:

(i) Comparing the hydrogenation of 1,1,1-trifluoroacetone and acetone it was observed that the former reacted promptly while the second was inert, and the calculation of adsorbed structures revealed that the former prefers a η^2(C,O) adsorption mode while the latter an η^1(O) adsorption mode.

(ii) The η^2(C,O) adsorption mode of a ketone has a strongly re-hybridized C=O moiety, and the carbonyl bond is elongated by ca. 0.1 Angstroms, thus being half way between the length of a ketone C=O and the length of the C—O bond of

an alcohol. In other words, η^2(C,O) is already activated and has a structure, which tends to that of an alcohol, while the η^1(O) adsorption mode is very similar to that of the species in vacuum.

Table 2

Calculated adsorption energies of **1a** and **5a** on a Pt 31 cluster, with respect to the most stable conformer (*s-trans* for **1a** and *s-cis* for **5a**)

Substrate	*s-cis* apical	*s-cis* non-apical	*s-trans* apical	*s-trans* non-apical
		η^2		
1a	27.7	31.2	27.2	27.8
5a	14.5	13.3	17.1	21.8
		η^1		
1a	15.8	–	18.2	–
5a	14.5	15.1	16.1	20.5

All energies are in kcal/mol.

Table 3

Calculated keto- and ester-carbonyl bond distances (Angstroms) of **1a** and **5a** in the free and adsorbed states described in Figs. 1–5

	Keto carbonyl	Ester carbonyl
Ethyl benzoylformate (**1a**)		
Free *s-trans*	1.22	1.21
Free *s-cis*	1.22	1.21
η^2 *s-cis* apical	1.22	1.22
η^2 *s-cis* non-apical	1.32	1.21
η^2 *s-trans* apical	1.22	1.22
η^2 *s-trans* non-apical	1.32	1.21
η^1 *s-cis* apical	1.21	1.21
η^1 *s-trans* apical	1.21	1.22
Ethyl mesithylglyoxylate (**5a**)		
Free *s-trans*	1.22	1.21
Free *s-cis*	1.22	1.21
η^2 *s-cis* apical	1.22	1.22
η^2 *s-cis* non-apical	1.32	1.21
η^2 *s-trans* apical	1.22	1.22
η^2 *s-trans* non-apical	1.32	1.21
η^1 *s-cis* apical	1.21	1.21
η^1 *s-cis* non-apical	1.24	1.21
η^1 *s-trans* apical	1.21	1.22
η^1 *s-trans* non-apical	1.24	1.22

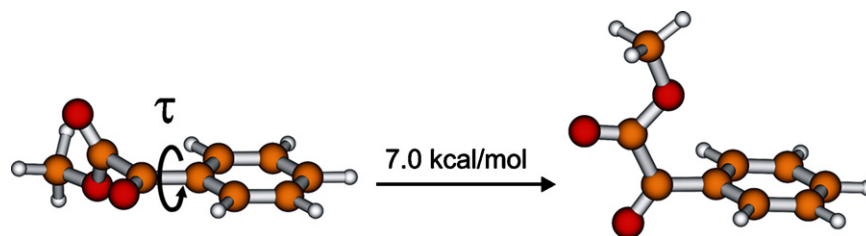In the table η^2 and η^1 refer to starting adsorption geometries.

Fig. 6. Rotation of the angle τ by 90° in **1a** implies a loss of energy of ca. 7.0 kcal/mol.

The arguments in favor of the second proposal are that experimental observations show that the predominant surface species after acetone adsorption is $\eta^1(O)$, while $\eta^2(C,O)$ is considered to be too strongly bound to the metal to be reactive. It should nonetheless here be briefly reminded that acetone does not undergo hydrogenation on platinum at a significant rate.

A recent publication on the mechanism of hydrogenation of 1-phenyl-1,2-propanedione showed a correlation between the $\eta^2(C,O)$ adsorption mode of the di-ketone and its conversion, apparently supporting the first hypothesis [13], and another recent work which focused on the enhancement of the regioselectivity in diketones hydrogenation in the presence of an amine also corroborated the $\eta^2(C,O)$ mechanism [12].

The catalytic experiments presented here show that the presence of aryl *o*-substituents in activated aromatic ketones reduces the reactivity dramatically in the hydrogenation on Pt. The modeling studies on the surface species show that the key effect of these *o*-substituents is the enhanced proportion of the $\eta^1(O)$ adsorption mode, relative to that of $\eta^2(C,O)$. While without *o*-substituents the $\eta^2(C,O)$ adsorption mode should dominate, the presence of *o*-substituents should reduce the surface coverage of all species, and especially greatly reduce the fractional coverage of $\eta^2(C,O)$ adsorption modes. Indeed, there seems to be a correlation between the adsorption mode of the ketone and the rate of hydrogen uptake, and this correlation supports a mechanistic picture where an $\eta^2(C,O)$ intermediate is required in order to have efficient transformation to the correspondent alcohol. Interestingly, a similar correlation between the energy of adsorption and the promptness to undergo saturation was observed in the hydrogenation of the aromatic moiety of differently substituted anisoles [26].

Nonetheless, the proposal by Willock and coworkers that $\eta^1(O)$ (or end-on) species are the reactive intermediates should not be completely ruled out. In their proposal the $\eta^1(O)$ adsorbed species bend down towards the surface thus reacting with adsorbed hydrogen. This reaction pathway is likely hindered by the presence of *o*-substituents at the phenyl moiety, as evidenced by the mentioned trapping of $\eta^1(O)$ species (Fig. 5) of **5a**. On the contrary, for **1a** $\eta^1(O)$ adsorbed structures are free to bend toward the surface, which could also explain their greater reactivity. A problem to the preceding explanation is that it would imply reaction intermediates having structures as the ones shown in Fig. 3, which are significantly less energetically bound to the metal (Table 2) and therefore, at equilibrium, should have negligible surface coverage. If a kinetic scenario is hypothesized, where $\eta^1(O)$ species as in Fig. 3 act as (fast reacting) reaction

intermediates without reaching equilibrium, also then a problem occurs: for non-adsorbed **1a** the keto-carbonyl moiety is on the same plane as the phenyl moiety, for both the *s-cis* and *s-trans* conformers. Formation of $\eta^1(O)$ species (Fig. 3) would imply that also in the liquid phase such conformer is present in significant amount. But if we consider the non-adsorbed molecule, rotation by 90° of the C–C bond (Fig. 6) to form a structure similar to the adsorbed one implies a loss of ca. 7.0 kcal/mol, which makes it an extremely low populated conformation also in a phase separate from the surface.

Finally, our combined experimental and theoretical investigation of the relation between the adsorption modes of activated aromatic ketones **1** and **5** and their reactivity towards hydrogenation led to a consistent result. Insertion of two *o*-substituents in the aromatic ring suppress $\eta^2(C,O)$ adsorption of the aromatic ketones and consequently the reactivity towards hydrogenation of the corresponding surface species disappears. The potential surface structure sensitivity, together with the possible influence of solvent, need to be taken into account to completely bridge the gap between the model calculations and the reactivity towards hydrogenation of these substrates on the supported catalyst. Work towards this aim is presently pursued in our laboratories.

4. Conclusions

Catalytic hydrogenation of various aromatic ketones activated by an ester group in α-position revealed that two aromatic substituents in *o*-position (substrates **4** and **5**) hinder the hydrogenation of the keto-carbonyl group on Pt/Al$_2$O$_3$. For comparison, in the absence of *o*-substituents (substrate **1**) the hydrogenation to the corresponding alcohol runs smoothly under mild conditions.

Theoretical calculations involving a model platinum(1 1 1) surface indicated that the presence of two *o*-substituents causes a large loss in the adsorption energy of the $\eta^2(C,O)$ adsorption mode with respect to the same molecule without such substitution. The loss of reactivity by insertion of two *o*-substituents could therefore be rationalized by a mechanistic hypothesis where the $\eta^2(C,O)$ adsorption mode plays a crucial role. According to this hypothesis, the keto-carbonyl moiety is first chemisorbed on the metal surface, thus undergoing bond elongation and re-hybridization, and in a second step reacts with surface hydrogen to form the alcohol. Although a complete simulation of the elementary steps would still be necessary to finally assert the most probable surface reaction pathway, the alternative mechanistic hypothesis based on the prominent role

of the $\eta^1(O)$ adsorbed keto-carbonyl species is challenged by the present results.

Acknowledgements

References

[1] A.B. Anton, N.R. Avery, B.H. Toby, W.H. Weinberg, J. Am. Chem. Soc. 108 (1986) 684.
[2] J.L. Davis, M.A. Barteau, Surf. Sci. 208 (1989) 383.
[3] C. Houtman, M.A. Barteau, J. Phys. Chem. 95 (1991) 3755.
[4] Z.M. Liu, M.A. Vannice, Surf. Sci. 316 (1994) 337.
[5] M. Mavrikakis, M.A. Barteau, J. Mol. Catal. A: Chem. 131 (1998) 135.
[6] R. Alcala, J. Greeley, M. Mavrikakis, J.A. Dumesic, J. Chem. Phys. 116 (2002) 8973.
[7] E.L. Jeffery, R.K. Mann, G.J. Hutchings, S.H. Taylor, D.J. Willock, Catal. Today 105 (2005) 85.
[8] A. Vargas, T. Bürgi, A. Baiker, J. Catal. 222 (2004) 439.
[9] M. Kraus, Adv. Catal. 29 (1980) 151.
[10] K. Tanaka, Stud. Surf. Sci. Catal. 27 (1986) 79.
[11] R. Hirschl, A. Eichler, J. Hafner, J. Catal. 226 (2004) 273.
[12] S. Diezi, D. Ferri, A. Vargas, T. Mallat, A. Baiker, J. Am. Chem. Soc. 128 (2006) 4048.
[13] V. Nieminen, A. Taskinen, M. Hotokka, D.Y. Murzin, J. Catal. 245 (2007) 228.
[14] A. Baiker, J. Mol. Catal. A: Chem. 115 (1997) 473.
[15] K.A. Avery, R. Mann, M. Norton, D.J. Willock, Top. Catal. 25 (2003) 89.
[16] D. Ferri, T. Bürgi, J. Am. Chem. Soc. 123 (2001) 12074.
[17] T. Bürgi, F. Atamny, R. Schlögl, A. Baiker, J. Phys. Chem. B 104 (2000) 5953.
[18] T. Bürgi, F. Atamny, A. Knop-Gericke, M. Havecker, T. Schedel-Niedrig, R. Schlögl, A. Baiker, Catal. Lett. 66 (2000) 109.
[19] J.M. Bonello, F.J. Williams, A.K. Santra, R.M. Lambert, J. Phys. Chem. B 104 (2000) 9696.
[20] J.M. Bonello, E.C.H. Sykes, R. Lindsay, F.J. Williams, A.K. Santra, R.M. Lambert, Surf. Sci. 482 (2001) 207.
[21] C. Kashima, Y. Shirahata, Y. Tsukamoto, Heterocycles 49 (1998) 459.
[22] X. Creary, M.E. Mehrsheikhmohammadi, S. McDonald, J. Org. Chem. 52 (1987) 3254.
[23] R. Hess, F. Krumeich, T. Mallat, A. Baiker, Catal. Lett. 92 (2004) 141.
[24] ADF2006.01, SCM, Theoretical Chemistry, Vrije Universiteit, Amsterdam, The Netherlands, http://www.scm.com.
[25] A. Vargas, T. Bürgi, A. Baiker, J. Catal. 226 (2004) 69.
[26] N. Bonalumi, A. Vargas, D. Ferri, A. Baiker, J. Phys. Chem. B 110 (2006) 9956.
[27] E. van Lenthe, E.J. Baerends, J.G. Snijders, J. Chem. Phys. 99 (1993) 4597.
[28] E. van Lenthe, E.J. Baerends, J.G. Snijders, J. Chem. Phys. 101 (1994) 9783.
[29] E. van Lenthe, A. Ehlers, E.J. Baerends, J. Chem. Phys. 110 (1999) 8943.
[30] E. van Lenthe, J.G. Snijders, E.J. Baerends, J. Chem. Phys. 105 (1996) 6505.
[31] E. van Lenthe, R. vanLeeuwen, E.J. Baerends, J.G. Snijders, Int. J. Quantum Chem. 57 (1996) 281.
[32] S.H. Vosko, L. Wilk, M. Nusair, Can. J. Phys. 58 (1980) 1200.
[33] A.D. Becke, Phys. Rev. A 38 (1988) 3098.
[34] J.P. Perdew, Phys. Rev. B 33 (1986) 8822.
[35] M.J.T. Frisch, G.W. Trucks, H.B. Schlegel, G.E. Scuseria, M.A. Robb, J.R. Cheeseman, J.A. Montgomery Jr., T. Vreven, K.N. Kudin, J.C. Burant, J.M. Millam, S.S. Iyengar, J. Tomasi, V. Barone, B. Mennucci, M. Cossi, G. Scalmani, N. Rega, G.A. Petersson, H. Nakatsuji, M. Hada, M. Ehara, K. Toyota, R. Fukuda, J. Hasegawa, M. Ishida, T. Nakajima, Y. Honda, O. Kitao, H. Nakai, M. Klene, X. Li, J.E. Knox, H.P. Hratchian, J.B. Cross, V. Bakken, C. Adamo, J. Jaramillo, R. Gomperts, R.E. Stratmann, O. Yazyev, A.J. Austin, R. Cammi, C. Pomelli, J.W. Ochterski, P.Y. Ayala, K. Morokuma, G.A. Voth, P. Salvador, J.J. Dannenberg, V.G. Zakrzewski, S. Dapprich, A.D. Daniels, M.C. Strain, O. Farkas, D.K. Malick, A.D. Rabuck, K. Raghavachari, J.B. Foresman, J.V. Ortiz, Q. Cui, A.G. Baboul, S. Clifford, J. Cioslowski, B.B. Stefanov, G. Liu, A. Liashenko, P. Piskorz, I. Komaromi, R.L. Martin, D.J. Fox, T. Keith, M.A. Al-Laham, C.Y. Peng, A. Nanayakkara, M. Challacombe, P.M.W. Gill, B. Johnson, W. Chen, M.W. Wong, C. Gonzalez, J.A. Pople, Gaussian 03, Revision C. 02, Gaussian, Inc., Wallingford, CT, 2004.
[36] A.D. Becke, J. Chem. Phys. 98 (1993) 5648.
[37] C.T. Lee, W.T. Yang, R.G. Parr, Phys. Rev. B 37 (1988) 785.
[38] B. Miehlich, A. Savin, H. Stoll, H. Preuss, Chem. Phys. Lett. 157 (1989) 200.
[39] S. Niwa, S. Imai, Y. Orito, Bull. Chem. Soc. Jpn. 4 (1982) 137.
[40] Y. Orito, S. Imai, S. Niwa, Bull. Chem. Soc. Jpn. 1 (1980) 670.
[41] A. Baiker, H.U. Blaser, in: G. Ertl, H. Knözinger, J. Weitkamp (Eds.), Handbook of Heterogeneous Catalysis, Wiley-VCH, Weinheim, 1997.
[42] M. Bartok, Curr. Org. Chem. 10 (2006) 1533.
[43] S. Diezi, S. Reimann, N. Bonalumi, T. Mallat, A. Baiker, J. Catal. 239 (2006) 255.
[44] M. Saeys, M.F. Reyniers, G.B. Marin, M. Neurock, J. Phys. Chem. B 106 (2002) 7489.
[45] C. Morin, D. Simon, P. Sautet, J. Phys. Chem. B 107 (2003) 2995.
[46] F. Mittendorfer, C. Thomazeau, P. Raybaud, H. Toulhoat, J. Phys. Chem. B 107 (2003) 12287.
[47] C. Morin, D. Simon, P. Sautet, J. Phys. Chem. B 108 (2004) 12084.
[48] G.A. Somorjai, Introduction to Surface Chemistry and Catalysis, Wiley, New York, 1994.